Double-strand DNA cleavage from photodecarboxylation of (μ-oxo)diiron(III) L-histidine complex in visible light

Mithun Roy, Tuhin Bhowmick, Suryanarayanarao Ramakumar, Munirathinam Nethaji, and Akhil R. Chakravarty*

Department of Inorganic and Physical Chemistry and Bioinformatics center, Department of Physics, Indian Institute of Science, Bangalore 560012, India

Supplementary Information

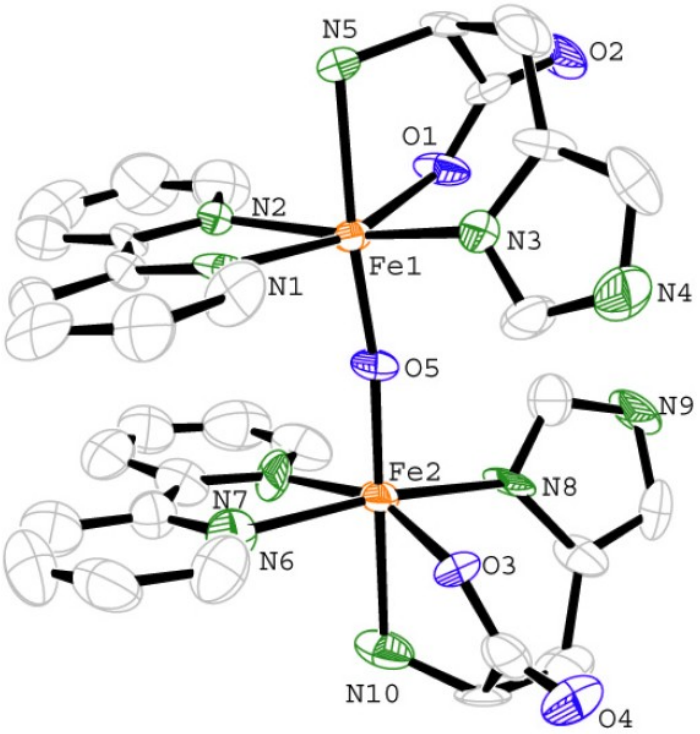

Fig. S1. The ORTEP view of the cationic complex of [{Fe(L-his)(bpy)}$_2$(μ-O)](ClO$_4$)$_2$·4H$_2$O (**1**·4H$_2$O) showing 50% probability thermal ellipsoids and the atom labelling scheme for the metal and hetero atoms. The hydrogen atoms are omitted for clarity.

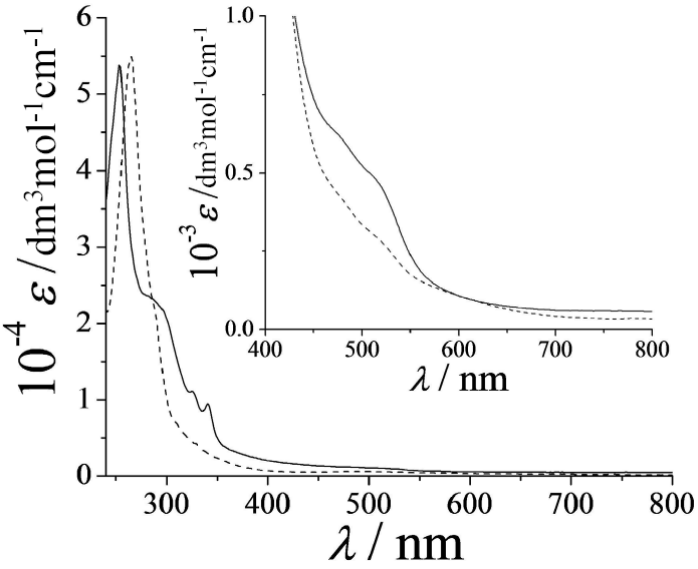

Fig. S2. The electronic spectra of the complexes **1** (- - -) and **2** (—) in Tris-HCl buffer (pH 7.2).

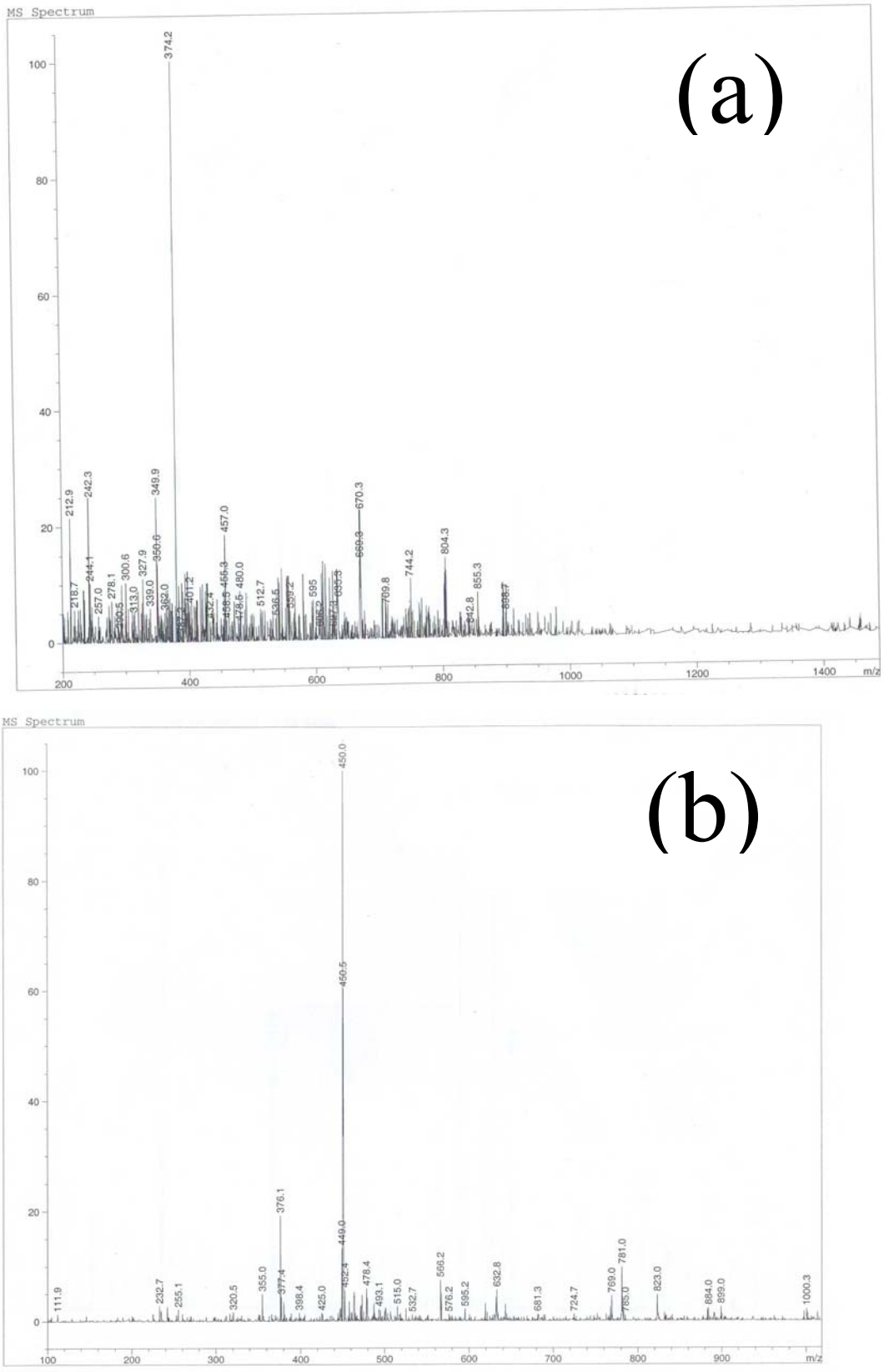

Fig. S3. (a) ESI-MS spectrum of **1** in H_2O showing the parent ion peak at m/z 374 $(M-2ClO_4)^{2+}$. (b) ESI-MS spectrum of **2** in H_2O showing the parent ion peak at m/z 450 $(M-2ClO_4)^{2+}$. The equipment used was of Bruker Daltonics make Esquire 300 Plus ESI Model.

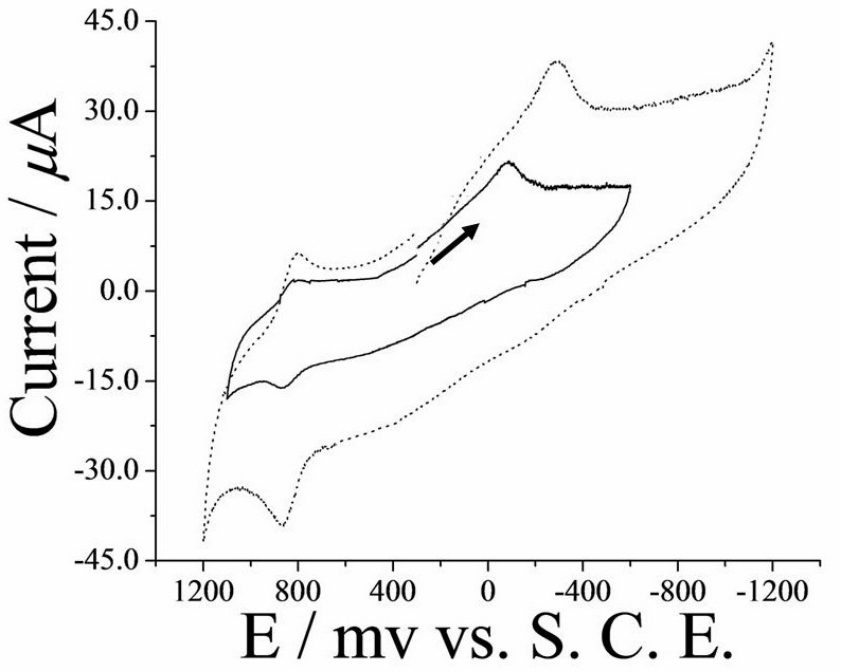

Fig. S4. The cyclic voltammetric responses of the complexes **1** (·····) and **2** (—) in water-0.1M KCl at the scan rate of 50 mVs^{-1} with reference to S. C. E. Both the complexes **1** and **2** display irreversible cyclic voltammetric responses at - 250 mV and - 50 mV respectively.

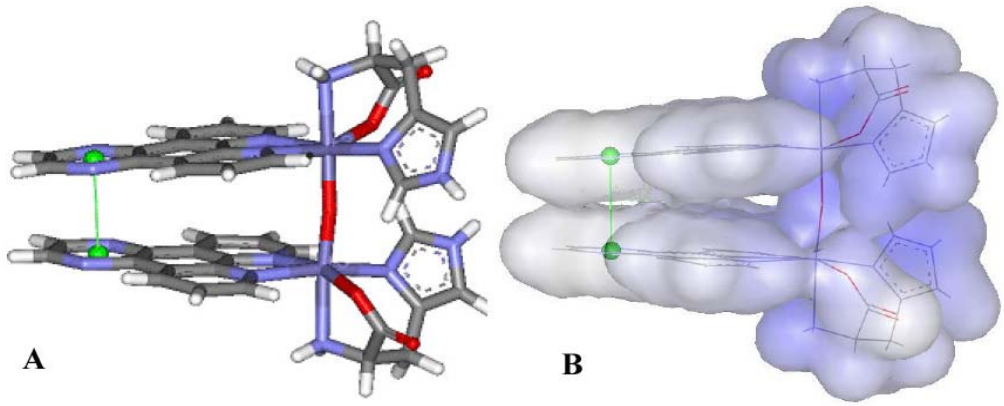

Fig. S5. (A) The dipyridoquinoxaline complex **2** in its original conformation as derived from model building (ring extension and energy minimization on the basis of the X-ray crystallographic structure of the 2,2'-bipyridine complex **1**. (B) van der Waals surface generated for complex **2** in its original conformation showing the tightly stacked rings. Model building and optimization was performed using the **DS Modelling 1.1 SBD, Model building and Energy minimization modules of Accelrys™ Software Package.** As a basic seed for the comparative model building, the X-ray crystallographic structure of the complex **1** was taken. After making the necessary changes like ring extension and cleaning the geometry, the model was subjected to energy minimization via Conjugate Gradient steps. The optimized model showed clear stacking interaction between the dpq rings.

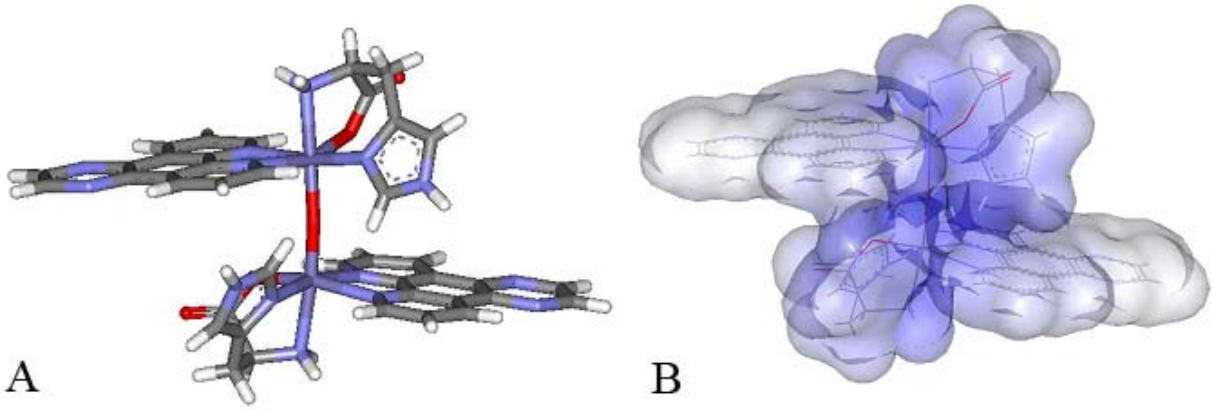

Fig. S6. (A) The complex **2** in its flipped conformation giving **2a** as derived from the best docked pose with DNA d(CGCGAATTCGCG)$_2$. (B) van der Waals surface generated for complex **2a** in its flipped conformation showing the opening of the stacked rings.

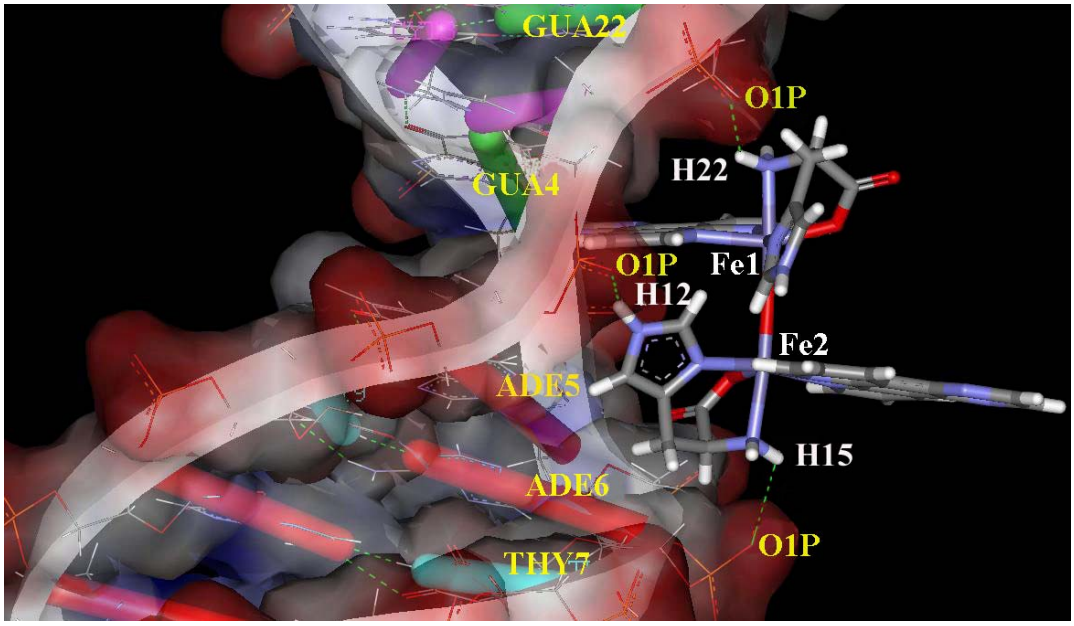

Fig. S7. Interaction of complex **2** with both the strands of DNA by formation of three H-bonds (**N21-H22** (complex)---**O 1P GUA22** (DNA-Chain B)], [**N11-H12** (**2**)---**O 1P CYT21** (DNA-Chain B)], [**N13-H15** (**2**)---**O 1P THY7** (DNA-Chain A)], through its minor groove binding approach. Corresponding H-bonds are shown in the **Table S1**.

Molecular docking calculation:

Molecular docking was performed using the **DS Modelling 1.2-SBD, Docking Module**, by **Accelrys™** Software. The CHARMm force-field was used for the metal complex in the input of the calculations. Due to the higher hybridization state of Fe^{3+} atom in the molecule, the correction of the partial charge distribution for all the atoms in the complex was done by following the output from *Gaussian 03*. The DNA crystal structure of the B-DNA dodecamer $d(CGCGAATTCGCG)_2$ (NDB code GDLB05), was downloaded from Protein Data Bank. In the docking analysis, the binding site was assigned across the entire minor and major grooves of the DNA molecule. The docking was performed to find the most stable and favorable orientation. The Docking options consists of the following steps: (i) Monte Carlo options: perform flexible fit; (ii) Thresholds for diversity of saved pose (defined by user to 2Å to scan through different conformations); (iii) Pose optimization done in two steps (a) Steepest descent minimization and (b) BFGS rigid body minimization; (iv) complex **2** internal energy optimization and filtering poses with short contacts (VDW and electrostatic energy calculated); and (v) Pose filtering and processing. Dock scores for conformations above energy 2 Kcal/mol were accepted. Clustering of poses using leader algorithm was done.

Dock score: Scoring for the docked poses were determined primarily using **Ludi score**, including five major contributions (a) contributions from ideal hydrogen bonds; (b) contributions from perturbed ionic interaction; (c) contributions from lipophilic interaction; (d) contribution due to the freezing of internal degrees of freedom; (e) contributions due to the loss of translational and rotational entropy of the ligand.

A second estimate of the Ludi score was obtained by changing the weights of the above contributors, while the weights are derived from Ludi score fitted to experimentally determined binding affinities. Correlation between Ludi score, dissociation constant (ki) and Gibbs free Energy (ΔG):

Score = 100 log ki

As, $\Delta G = -RT \ln ki = -2.303\ RT \log 10(ki)$
Score = -73.33 mol/Kcal·ΔG (T= 298 K)

Docking Results:
This optimum docking state with the highest energy stabilization was obtained in a two stage docking, where following the previously mentioned steps the initial docking was performed. After the thorough analysis of different docked poses and the corresponding metal complex **2** conformations, the second stage of docking was performed in an energy profile guided manner depending upon the best binding trends using the top scored conformations of the ligand obtained as outputs from the first stage docking. Finally, the most favorable docked pose for the complex **2** was obtained as shown in **Fig. S6** (vide text), revealed by calculated free energy of **-6.248** Kcal M^{-1}. The most interesting observation is that in its optimal binding conformation, complex **2** acquires a flipped conformation, shown as **2a** in Scheme 1, in which its two dpq rings flips apart (as described in **Fig. S5A**). In the mentioned state, complex **2** approaches DNA through the minor groove and interacts through three H–bond formation involving three backbone oxygen atoms from including both the strands. This interaction goes appropriately with the experimental findings as DNA cleavage study clearly indicates cleavage of double strand. Additionally, the complex **2**-DNA interaction gets an additional stabilization via partial intercalation of one of the dpq rings of complex **2** with DNA base pairs (as explained in **Fig. S7**). The detailed analysis of the docked structure reveals the necessity of the flipped state of complex **2** as without this, due to steric hindrance, the docking cannot be optimal (as in the original state reported from energy minimized model on the basis of crystal structure of complex **1**, the inter-planar separation between the two dpq ring systems is clearly inadequate for incorporation into the DNA base steps allowing the optimal binding interaction).
The partial stacking information found from docking study has also been approved by experimental evidence from DNA melting point elevation.

Calculation of energy instability in the flipped conformation:
The instability of complex **2** is due to flipped conformation, contributed mainly from bond angle distortion, improper dihedrals, as well as breaking of stacking interaction which stabilizes the orientation in the original complex **2**.
Energy change (ΔE) due to conformational change of complex is calculated as $\Delta E_{(conformation)}$ = [Energy of Docked Conformation (Flipped state) of complex **2a** – Energy of Original modelled complex **2** structure (Stacked state)]; which was found to be +**45.9** cal M^{-1} **(= 0.0459** Kcal M^{-1}**),** indicating relative instability of the flipped state**.**

Overall system stability is through intermolecular interaction after binding to DNA:
Energy stabilization due to mainly H-bonding interaction, electrostatic interaction, and stacking interaction with the DNA as calculated from the docking study refers to a Ludi Score of 458.1, referring to a final stabilization energy of the system as - 6.248 Kcal M^{-1}. This implies, the energy instability is resulted by conformational changes to the flipped state of the complex in conformation 2a (scheme 1) is very well compensated due to the enhancement of intermolecular DNA-complex 2a interaction in the flipped state, as the flipping of the dpq rings (shown in 2a) with respect to one another provides the possibility of entering of one dpq ring in-between the base pairs (Cyt 21—Gua 4 and

Thy20—Ade 5) for partial intercalation resulting in more favourable binding in the complex 2's minor groove approach.

H-bonding interaction data for the docked pose of **2a** with d(CGCGAATTCGCG)$_2$ [a]

H bonding Details For 2a			
Donor group (Y-H)	**Acceptor group Z**	**Distance [Y → Z] (Å)**	**Angle Y--^H····Z**
N21-H22 (complex **2a**)	**O 1P GUA22** (DNA-Chain B)	2.54	134.2 °
N11-H12 (complex **2a**)	**O 1P CYT21** (DNA-Chain B)	2.79	154.7°
N13-H15 (complex **2a**)	**O 1P THY7** (DNA-Chain A)	3.49	119.7°

[a] Donor group is Y and acceptor group is Z in the hydrogen bond (Y-H • • • Z)

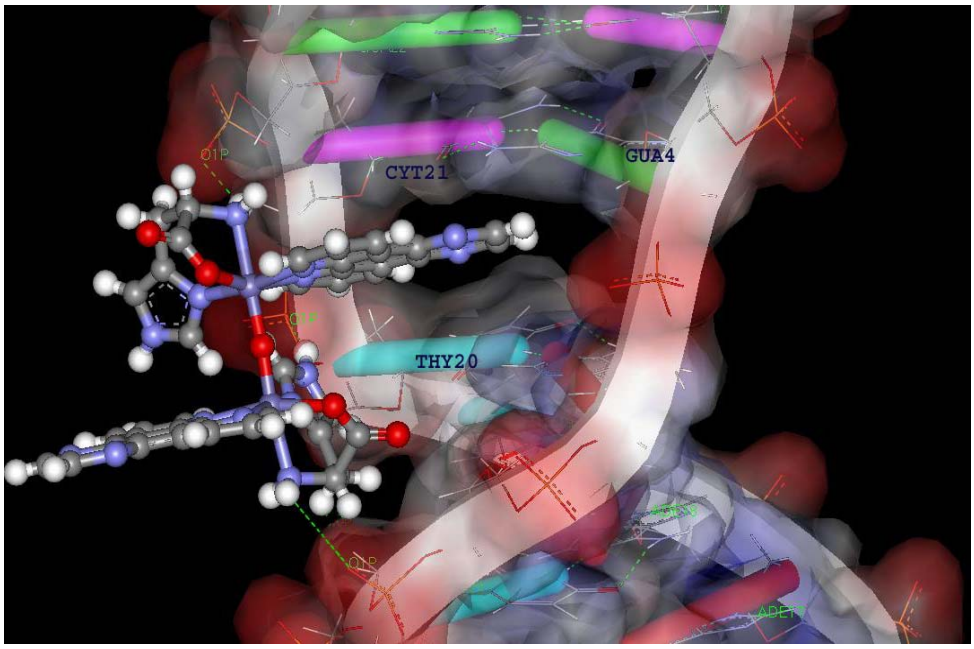

Fig. S8. Partial intercalation of dpq ring of complex **2** in the flipped state with DNA **d(CGCGAATTCGCG)$_2$**.The dpq ring (upper) of the complex (in **2a** conformation) into the DNA bases Cyt 21, and Thy 20, resulting in an intercalation cavity* formation in between the base pairs Cyt 21—Gua 4 and Thy20—Ade 5.

*[As the Docking module primarily imparts ligand flexibility and by and large considers the receptor macromolecule as a rigid entity, to impart partial flexibility to the docking site of the receptor (DNA), local distortion in the intercalation site was enhanced using the program NAMOT (Nucleic acid modelling tool; Theoretical Biology and Biophysics (T-10), Theoretical Division, Los Alamos National Laboratory, Los Alamos, NM 87545, USA), to provide a more realistic docking environment.]

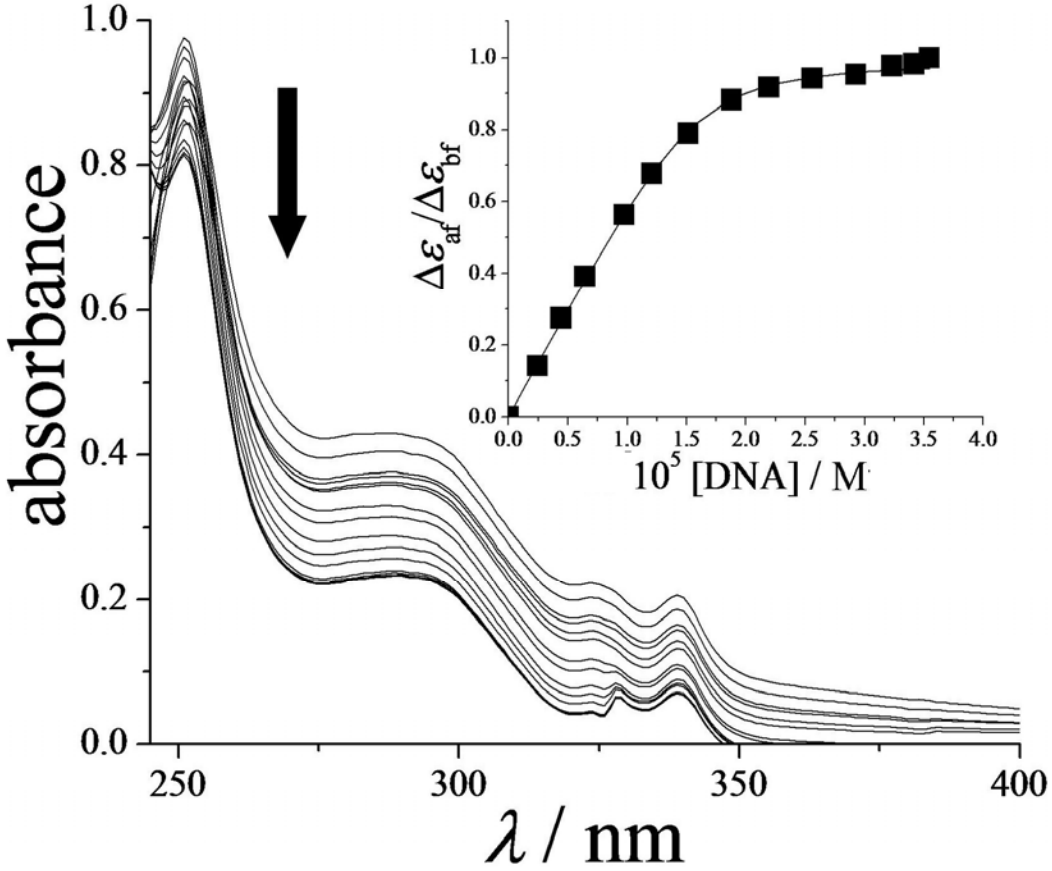

Fig. S9. Spectral traces showing the effect of addition of CT DNA (130 μM NP) to a 30 μM complex solution in Tris-HCl buffer (pH 7.2). The inset shows the MvH plot ($\Delta\varepsilon_{af}/\Delta\varepsilon_{bf}$ vs. [DNA]). The binding constant value (K) value is obtained by fitting non linearly the McGhee-von Hippel equation using the expression of Bard and coworkers, $C_b = (b - (b^2 - 2K^2C_t[\text{DNA}]/s)^{1/2})/2K$, $b = 1 + KC_t + K[\text{DNA}]/2s$, where K is the microscopic binding constant for each site, C_b is the concentration of the DNA bound complex, C_t is the total concentration of the metal complex, and s is the site size (in base pairs) of the metal complex interacting with the DNA, ε_f, ε_a and ε_b are respectively the molar extinction coefficients of the free complex in solution, complex bound to DNA at a definite concentration and the complex in completely bound form with CT DNA. Ref: J. D. McGhee and P. H. von Hippel, *J. Mol. Biol.*, 1974, **86**, 469; M. T. Carter, M. Rodriguez and A. J. Bard, *J. Am. Chem. Soc.*, 1989, **111**, 8901.

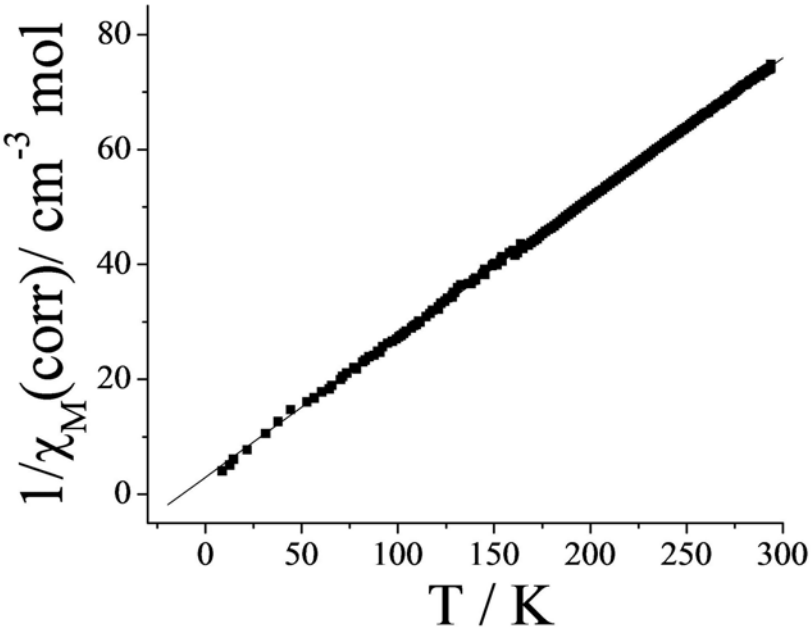

Fig. S10. Variable temperature magnetic susceptibility data for complex **2** giving a θ value of -20 K from the fitting. The data in the range of 300-20 K for polycrystalline sample of the complex were obtained using Model 300 Lewis-coil-force magnetometer of George Associates Inc. (Berkeley, USA) make. $Hg[Co(NCS)_4]$ was used as a standard. Experimental susceptibility data were corrected for diamagnetic contributions. Ref: O. Khan, *Molecular Magnetism*, VCH, Weinheim, 1993.

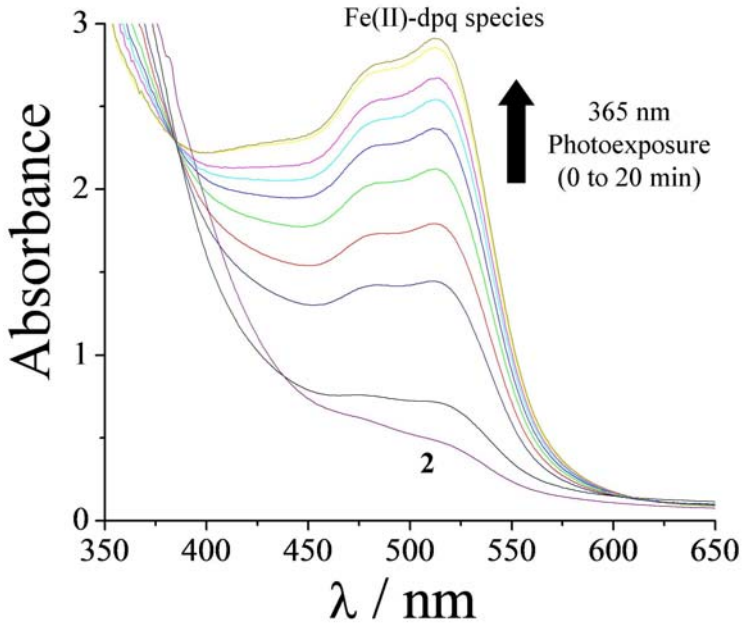

Fig. S11. Spectral traces showing the enhancement of the Fe(II)-dpq (LMCT) band intensity on photoexposure of the complex **2** at 365 nm for a duration of 20 min. The Fe(II)-dpq species is proposed to form from a decarboxylation reaction involving the Fe(III)-histidine moiety.

Table S1. Selected bond distances (Å) and bond angles (°) data for the complex **1**·4H_2O.

Fe(1) – O(5)	1.765(12)	Fe(2) – O(5)	1.801(12)
Fe(1) – O(1)	2.046(8)	Fe(2) – O(3)	1.989(9)
Fe(1) – N(3)	2.111(12)	Fe(2) – N(8)	2.090(10)
Fe(1) – N(2)	2.158(10)	Fe(2) – N(10)	2.164(11)
Fe(1) – N(1)	2.159(10)	Fe(2) – N(6)	2.164(11)
Fe(1) – N(5)	2.227(10)	Fe(2) – N(7)	2.179(13)
O(5) – Fe(1) - O(1)	98.9(4)	O(5) – Fe(2) – O(3)	104.3(4)
O(5) – Fe(1) – N(3)	93.6(4)	O(5) – Fe(2) – N(8)	94.9(4)
O(1) – Fe(1) – N(3)	90.7(4)	O(3) – Fe(2) – N(8)	90.1(4)
O(5) – Fe(1) – N(2)	96.9(4)	O(5) – Fe(2) – N(10)	178.1(4)
O(1) – Fe(1) – N(2)	94.8(4)	O(3) – Fe(2) – N(10)	77.3(4)
N(3) – Fe(1) – N(2)	167.3(4)	N(8) – Fe(2) – N(10)	84.0(4)
O(5) – Fe(1) – N(1)	96.1(4)	O(5) – Fe(2) – N(6)	94.0(4)
O(1) – Fe(1) – N(1)	162.4(4)	O(3) – Fe(2) – N(6)	91.7(4)
N(3) – Fe(1) – N(1)	97.4(4)	N(8) – Fe(2) – N(6)	170.2(4)
N(2) – Fe(1) – N(1)	74.3(4)	N(10) – Fe(2) – N(6)	87.0(5)
O(5) – Fe(1) – N(5)	174.1(4)	O(5) – Fe(2) – N(7)	93.5(4)
O(1) – Fe(1) – N(5)	75.8(4)	O(3) – Fe(2) – N(7)	158.8(4)
N(3) – Fe(1) – N(5)	84.0(4)	N(8) – Fe(2) – N(7)	100.0(5)
N(2) – Fe(1) – N(5)	86.2(4)	N(10) – Fe(2) – N(7)	85.1(5)
N(1) – Fe(1) – N(5)	89.5(4)	N(6) – Fe(2) – N(7)	75.4(5)
Fe(1) – O(5) – Fe(2)	171.8(5)		

Table S2. H-bonding interaction table for the docked pose of **2a** with d(CGCGAATTCGCG)$_2$[a]

H bonding Details For the complex in 2a conformation			
Donor group (Y-H)	**Acceptor group Z**	**Distance [Y → Z] (Å)**	**Angle Y---^H···Z**
N21-H22 (complex **2a**)	**O 1P GUA22** (DNA-Chain B)	2.54	134.2°
N11-H12 (complex **2a**)	**O 1P CYT21** (DNA-Chain B)	2.79	154.7°
N13-H15 (complex **2a**)	**O 1P THY7** (DNA-Chain A)	3.49	119.7°

[a] Donor group is Y and acceptor group is Z in the hydrogen bond (Y-H • • • Z)